NeuroImage 297 (2024) 120756

Contents lists available at ScienceDirect

NeuroImage

journal homepage: www.elsevier.com/locate/ynimg

Are older adults less generous? Age differences in emotion-related social decision making

Hong-Zhou Xu [a], Xue-Rui Peng [b,c,d], Shen-Yin Huan [a], Jia-Jie Xu [a], Jing Yu [a,*], Qing-Guo Ma [e,f]

[a] Faculty of Psychology, Southwest University, Chongqing 400715, China
[b] Faculty of Psychology, Technische Universität Dresden, Dresden 01062, Germany
[c] Centre for Tactile Internet with Human-in-the-Loop, Technische Universität Dresden, Dresden 01062, Germany
[d] Max Planck Institute for Human Cognitive and Brain Sciences, Leipzig 04103, Germany
[e] Neuromanagement Laboratory, School of Management, Zhejiang University, Hangzhou 310058, China
[f] Institute of Neural Management Sciences, Zhejiang University of Technology, Hangzhou 310014, China

ARTICLE INFO

Keywords:
Social decision making
Aging
Dictator game
Representational similarity analysis
Neural pathways

ABSTRACT

In social interaction, age-related differences in emotional processing may lead to varied social decision making between young and older adults. However, previous studies of social decision making have paid less attention to the interactants' emotions, leaving age differences and underlying neural mechanisms unexplored. To address this gap, the present study combined functional and structural magnetic resonance imaging, employing a modified dictator game task with recipients displaying either neutral or sad facial expressions. Behavioral results indicated that although older adults' overall allocations did not differ significantly from those of young adults, older adults' allocations showing a decrease in emotion-related generosity compared to young adults. Using representational similarity analysis, we found that older adults showed reduced neural representations of recipients' emotions and gray matter volume in the right anterior cingulate gyrus (ACC), right insula, and left dorsomedial prefrontal cortex (DMPFC) compared to young adults. More importantly, mediation analyses indicated that age influenced allocations not only through serial mediation of neural representations of the right insula and left DMPFC, but also through serial mediation of the mean gray matter volume of the right ACC and left DMPFC. This study identifies the potential neural pathways through which age affects emotion-related social decision making, advancing our understanding of older adults' social interaction behavior that they may not be less generous unless confronted with individuals with specific emotions.

1. Introduction

Social interaction is critical for maintaining health and happiness throughout the life (Fratiglioni et al., 2004; Lockwood et al., 2021). To better interact with others, people need to perceive and process others' emotions, and integrate social and emotional information in order to regulate their behavior in social interactions in a timely manner, for example, by offering help to a person who is sad. Previous meta-analyses have shown that older adults are less accurate than young adults at identifying facial expressions, especially negative emotions (Gonçalves et al., 2018; Ruffman et al., 2008). However, previous studies of social decision making have paid less attention to the emotions of interactants, leaving age-related differences and underlying neural mechanisms untested. In the context of social interaction, it has been shown that older adults' decision making is less sensitive to emotions under certain circumstances when interacting with socially disadvantaged individuals, such as those with sad emotions (Hettich et al., 2018; Wiepking and James, 2013). It remains unclear whether this is due to age-related changes in the processing of others' emotions, resulting in a lack of sensitivity in value allocation, or whether they undergo changes in the integration of social and emotional information during value-based social decision making, resulting in a decrease in emotion-related generosity. Addressing this question will provide insight into the neural processes of emotion-related social decision making, thereby advancing our understanding of the underlying mechanisms of changes in older adults' social interaction behavior.

Aging leads to significant changes in the function and structure of brain regions underlying emotion processing (Gunning-Dixon et al.,

* Corresponding author at: Faculty of Psychology, Southwest University, Tiansheng Road, Beibei District, Chongqing 400715, China.
E-mail address: helen12@swu.edu.cn (J. Yu).

https://doi.org/10.1016/j.neuroimage.2024.120756
Received 28 May 2024; Received in revised form 9 July 2024; Accepted 24 July 2024
Available online 27 July 2024

2003; Mather, 2012, 2016), among which the anterior cingulate cortex (ACC) and insula, as core nodes of the salience/midcingulo-insular network (Menon and Uddin, 2010; Toga, 2015; Ziaei et al., 2021), play critical roles in emotion-related social decision making (Kanel et al., 2019; Rogers-Carter and Christianson, 2019; Ziaei et al., 2021). The ACC has been implicated in processing the emotions and motivations of others (Apps et al., 2016; Meng et al., 2023). The insula is involved in the subjective experience of emotions (Namkung et al., 2017; Pavuluri and May, 2015; Singer et al., 2009), as well as the perception and processing of social cues, such as facial expressions and vocal tones (Kanel et al., 2019; Mauchand and Zhang, 2023; Rogers-Carter and Christianson, 2019; Schirmer and Adolphs, 2017; Zhang et al., 2019). It also interacts with the frontotemporal network, allowing individuals to consciously acquire perceived signals and integrate them into more complex emotional and social cognitive processes (Adolfi et al., 2017). However, compared to young adults, older adults have shown altered or even the opposite patterns of ACC activation when processing different emotional stimuli (Leclerc and Kensinger, 2008). Besides, gray matter volume (GMV) and white matter integrity of the insula decrease with age, which is associated with decreased signal reactivity to emotional stimuli and reduced ability to understand emotions (Dobrushina et al., 2020; Niu et al., 2024). These changes in the ACC and insula of older adults may lead to challenges in processing others' emotions in emotion-related social decision making(Chen et al., 2014; Orlando and Filippini, 2024; Ziaei et al., 2021).

Furthermore, brain regions that support the integration of social and emotional information in value-based social decision making also showed age-related functional and structural changes, such as the dorsomedial prefrontal cortex (DMPFC; Allard and Kensinger, 2014; Jobson et al., 2021; Sun et al., 2016). As a key node of cognitive empathy network (Shamay-Tsoory, 2011; Wever et al., 2021), the DMPFC integrates social and emotional information (Ferrari et al., 2016; Frazier et al., 2019; Izuma and Adolphs, 2013; Kensinger and Ford, 2021; Martin et al., 2017; Wagner et al., 2016) to empathize with the pain and misfortune of others (Ding et al., 2020; Krishnan et al., 2016; Wever et al., 2021). In young adults, those with higher DMPFC activation not only offer more help when witnessing others in pain, but also donate more money after viewing photos of disaster victims (Bruneau et al., 2012; Mathur et al., 2010). Furthermore, the activity in the DMPFC encodes relative subjective value and generalizes across self and others and across tasks, shedding light on how the DMPFC may use task-invariant mechanisms to compute relative subjective value for self and others (Piva et al., 2019; Tomova et al., 2020). Age-related changes in the DMPFC may further affect older adults' integration of social and emotional information to empathize with others and calculate relative subjective value for self and others (Cassidy et al., 2013; Ferrari et al., 2016; Frazier et al., 2019; Piva et al., 2019; Tomova et al., 2020).

In this study, we recruited young and older adults to perform a modified dictator game task with neutral and sad recipients in functional magnetic resonance imaging (fMRI) scanner to examine the age differences in emotion-related social decision making. To investigate how age impacts the neural representations of recipients' emotions, we first used representational similarity analysis (RSA) to compare the neural representations of recipients' emotions in young and older adults and to identify brain regions with age-related differences. The advantage of RSA in fMRI over univariate activation analysis is its ability to incorporate multivoxel patterns, allowing for a more nuanced understanding of brain activity (Dimsdale-Zucker and Ranganath, 2018; Popal et al., 2019). RSA can be used not only to reflect the relative dissimilarity structure of the relationships between all studied stimulus pairs by constructing stimulus representation dissimilarity matrices (RDMs), but also to reflect the dissimilarity of the multivoxel patterns evoked between stimulus pairs at the neural level by constructing neural RDMs, and to compare stimulus RDMs with neural RDMs to test which brain regions are better able to represent stimulus patterns (Levine and Schwarzbach, 2021; Popal et al., 2019). We hypothesized that older adults would show decreased neural representations of recipients' emotions in the ACC, insula, and DMPFC compared to young adults. Second, we examined differences in the GMV of those brain regions where age-related differences in RSA were found. We hypothesized that GMV in the ACC, insula, and DMPFC would be lower in older adults than in young adults. Third, serial mediation analyses were used to identify potential neural pathways for the effect of age on allocations. We hypothesized that the emotions processed by the ACC and insula may be further integrated by the DMPFC, completing the calculation of relative subjective value for self and others to guide allocation behavior. Thus, age might cause changes in emotion-related social decision making through serial mediation effects of function (i.e., neural representations) and structure (i.e., GMV) of the ACC and DMPFC or the insula and DMPFC.

2. Methods

2.1. Participants

A total of 68 right-handed participants with no history of psychiatric or neurological diseases participated in the study, among which 32 young adults were recruited from Southwest University and 36 older adults were from local communities. Older adults were independent community-dwelling adults whose Mini-mental State Examination (MMSE) scores were above 26. Due to excessive head movements (i.e., translation > 3 mm or rotation $> 3^{\circ}$ or mean framewise displacement (FD) > 0.3), one young adult and four older adults were excluded from the following analyses. As a result, we included 63 participants, with 31 young adults (aged 18~24 years) and 32 older adults (aged 59~78 years) in data analysis respectively. Young and older adults were matched for sex and subjective dispositional empathy measured by the Interpersonal Reactivity Index-C (Zhang et al., 2010), while older adults were generally less educated (Table 1). Given the significant difference in years of education between young and older adults, it is controlled for as a covariate in all analyses unless otherwise specified.

This study was approved by the Ethics Committee of Southwest University to be in accordance with the Declaration of Helsinki (H17014). Participants provided informed consent prior to the experiment. Each participant received monetary reward for participation in the study.

2.2. Experimental materials

In this study, we used the Chinese Facial Affective Picture System (CFAPS; Gong et al., 2011) as our source of experimental stimuli. We randomly selected 80 neutral and 80 sad face pictures that balanced the sex. Sad face pictures were included because sadness may be more likely to motivate altruistic behavior (Small and Verrochi, 2009; Van Kleef and Lelieveld, 2022; Xiao et al., 2021), and neutral face pictures were

Table 1
Demographic information and statistical inference.

	YA ($n = 31$) $M \pm SD$	OA ($n = 32$) $M \pm SD$	t	p
Age (years)	20.65 ± 1.60	67.59 ± 3.96	−62.05	<0.001
Sex (M/F)	10/21	13/19	0.48[a]	0.49
Education (years)	14.71 ± 1.64	9.88 ± 2.71	8.60	<0.001
MMSE (0–30)	–	28.47 ± 1.48	–	–
IRI-C[b]				
Perspective taking (0–20)	10.29 ± 3.49	11.63 ± 3.29	−1.56	0.12
Personal distress (0–20)	9.42 ± 4.59	7.88 ± 5.20	1.25	0.22
Fantasy scale (0–24)	11.61 ± 3.20	12.16 ± 4.24	−0.57	0.57
Empathetic concern (0–24)	11.71 ± 3.22	11.78 ± 3.13	−0.09	0.93

Note: [a] χ^2 test value; YA, young adults; OA, older adults; M, male, F, female; MMSE, Mini-mental State Examination, [b] IRI-C, Interpersonal Reactivity Index-C.

included as a control condition. Since the CFAPS database contained only young adult faces, we used Facelab (https://facelab.mobi/) to transform half of the selected pictures, both neutral and sad faces, into older faces. The consideration for the inclusion of older face pictures was that the participants included older individuals, which can balance out the age effect of stimuli. To refine our stimuli, a separate group of 11 older adults were recruited to rate the valence, arousal, and age of all face pictures. Selecting older adults to rate the face pictures ensured that the selected face pictures were more likely to evoke emotional experiences in older adults. Valence and arousal scores were rated on a 9-point scale, with higher valence scores indicating more positive, lower valence scores indicating more negative, and scores closer to 5 indicating more neutral. Age was rated over a range of 10–90 years. Using valence scores as the primary indicator, the pictures with the lowest mean valence scores were chosen as the sad pictures, while the pictures with the mean valence scores closest to 5 were chosen as the neutral pictures. A total of 88 face pictures were selected, comprising 22 pictures each of young neutral faces, young sad faces, older neutral faces, and older sad faces, respectively: 1) the emotional valence scores of the sad faces were significantly lower than that of the neutral faces ($t_{(86)} = -25.10$, $p < 0.001$); 2) the emotional arousal scores of sad faces were significantly higher than that of neutral faces ($t_{(86)} = 5.10$, $p < 0.001$); 3) the ages of older faces were significantly higher than that of young faces ($t_{(86)} = 34.34$, $p < 0.001$). Of the 88 face pictures selected, 8 pictures were used in the practical experimental task and 80 pictures were used in the formal experimental task.

2.3. Experimental task

We adapted the dictator game task (Brocklebank et al., 2011; Charness and Rabin, 2002) to investigate how recipients' facial emotions (sad vs. neutral) influence the social decision making of young and older adults. Specifically, participants were asked to perform a money allocation task with other players in the fMRI scanner. To simulate a realistic social context, participants were told that the other players were engaged via the Internet. There were two roles in the task, one was the "allocator", and the other was the "recipient". In each round, the allocator was required to allocate ¥ 10 between themselves and the recipient, deciding how much to allocate to the recipient, while keeping the remaining amount reserved for themselves. Recipients had no choice but to accept the offer. Before each allocation, the allocators were shown face pictures of the recipient showing either a neutral or sad emotion. Although participants were only assigned the role of allocator, they were told that the role was randomly selected. To further increase participants' involvement in the task, they were informed that the amount they kept in a random round was related to the monetary reward of the

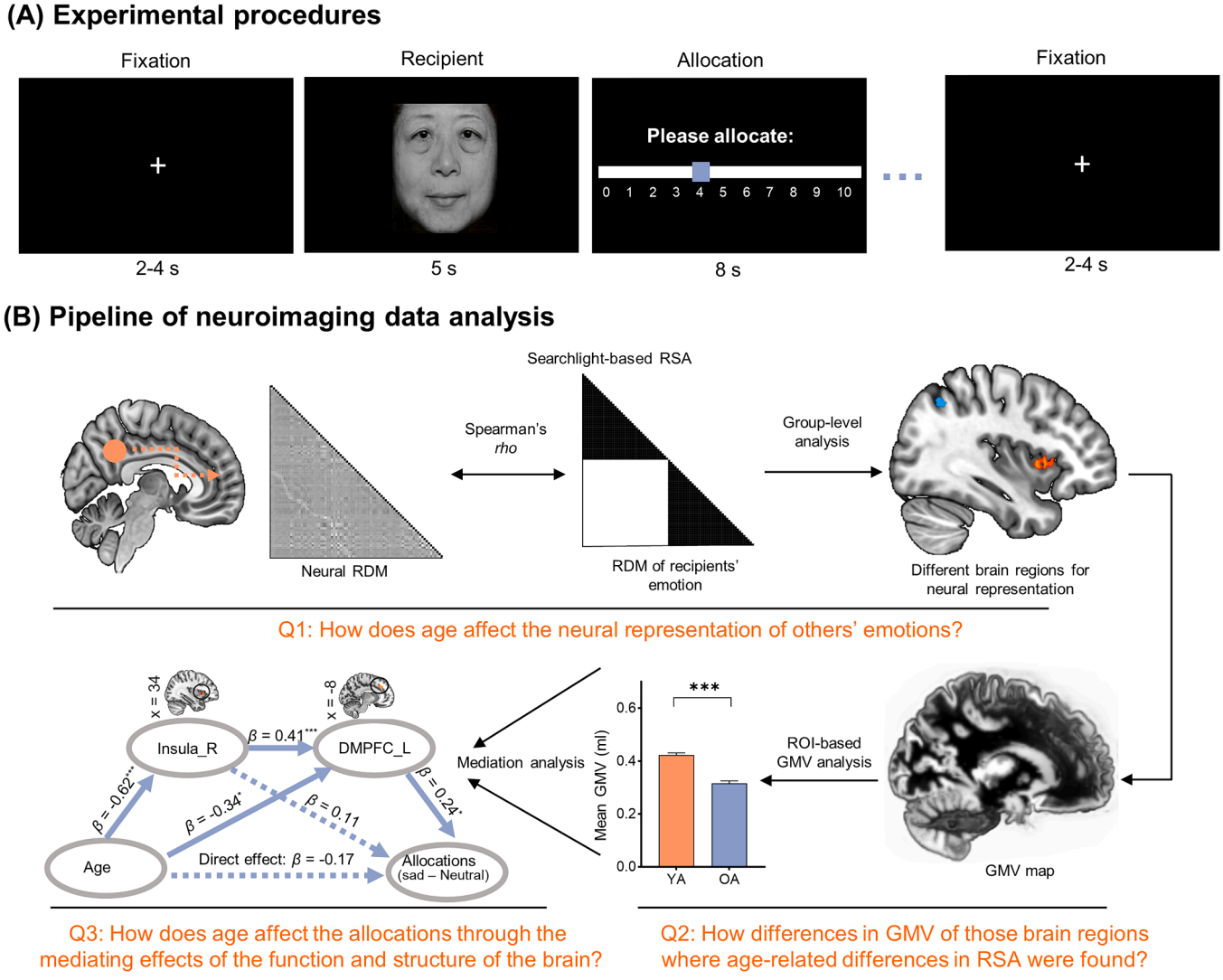

Fig. 1. (A) The experimental procedure and types of recipients. (B) The pipeline of neuroimaging data analysis. RSA, representational similarity analysis; RDM, representational dissimilarity matrix; GMV, gray matter volume; ROI, region of interest.

experiment.

Participants were first required to complete an 8-trial practice session (with different face pictures for each trial) outside the fMRI scanner to familiarize themselves with the experimental procedures. After practice, participants completed two runs of the formal experimental tasks in the fMRI scanner, each run containing 40 face pictures, with each picture presented pseudo-randomly once. As shown in Fig. 1A, in each trial, the fixation was first presented as a jitter for 2–4 s (mean interval of 3 s), followed by the recipient's picture for 5 s. The allocation phase lasted 8 s, during which participants could move the position of the slider by pressing the "2″ key on the left hand and the "3″ key on the right hand. The starting positions of the sliders were randomized on each trial. In addition, participants were instructed that if the starting position of the slider was the position of their choice, they also had to press the corresponding key on their left hand and then the corresponding key on their right hand to move the slider one space to the left and then back to the starting position. This was done to ensure that the slider position was chosen by them, rather than caused by distraction or other reasons. The presentation of the experimental materials and the recording of the participants' responses were performed by E-Prime 2.0 (http://www.pstnet.com/eprime.cfm; Psychology Software Tools, Inc., Pittsburgh, PA, RRID: SCR_009567).

After completing the main task, participants were asked to complete an out-of-scanner allocation questionnaire to verify their allocation, as shown in Figure S1. Allocation amounts and types of recipients were the same as in the scanner. This procedure was designed to examine the effectiveness of picture stimuli by comparing the consistency between the results of the picture stimuli and the text description. Two older adults did not complete the questionnaire.

2.4. Behavioral data analysis

We used the R package afex (https://cran.r-project.org/web/packages/afex/index.html) to perform the 2 (age: young adults vs. older adults) × 2 (recipients' emotions: neutral vs. sad) repeated measures analysis of covariance (ANCOVA) on participants' mean allocations in the experimental task and the out-of-scanner allocation questionnaire. Trials in which participants did not respond to keypresses were excluded from data analyses for in-scanner data. Overall, only 0.7 % of the trials in older adults and 1.4 % in young adults were excluded.

2.5. MRI data acquisition

Structural and functional images were acquired using a 3T Siemens Prisma MRI system at the Brain Imaging Center, Southwest University. Functional images were acquired using a gradient echo planar imaging (EPI) sequence with the following parameters: repetition time (TR) = 2000 ms, echo time (TE) = 30 ms, field of view (FOV) = 224 × 224 mm^2, acquisition matrix = 112 × 112, flip angle = 90°, 62 axial slices, slice thickness = 2.00 mm, acquisition matrix = 64 × 64, voxel size = 2.00 × 2.00 × 2.30 mm^3, phase encoding direction = $P >> A$, and multiband factor = 2. Participants were scanned for two task-state runs, each consisting of 324 TRs. High-resolution T1-weighted (T1w) structural images were acquired with the following parameters: TR = 2530 ms, TE = 2.98 ms, flip angle = 7°, FOV = 256 × 256 mm2, voxel size = 0.5 × 0.5 × 1 mm^3, phase encoding direction = $A >> P$. Participants were scanned for 192 TRs of structural images.

2.6. MRI data preprocessing

2.6.1. Anatomical data preprocessing

The T1w image was corrected for intensity non-uniformity (INU) using N4BiasFieldCorrection (Tustison et al., 2010), distributed with ANTs 2.3.3 (Avants et al., 2008, RRID: SCR_004757), and used as the T1w-reference for the subsequent workflow. The T1w-reference was then skull-stripped using a Nipype implementation of the antsBrainExtraction.sh workflow (from ANTs), with OASIS30ANTs as the target template. Brain tissue segmentation of cerebrospinal fluid (CSF), white matter (WM), and gray matter (GM) was performed on the brain-extracted T1w using fast (FSL 5.0.9, RRID: SCR_002823; Zhang et al., 2001). Volume-based spatial normalization to two standard spaces (MNI152NLin6Asym, MNI152NLin2009cAsym) was performed by nonlinear registration with ants Registration (ANTs 2.3.3), using brain-extracted versions of both T1w reference and the T1w template.

2.6.2. Functional data preprocessing

The following preprocessing was performed for each of the 2 BOLD runs found per participant. First, a reference volume and its skull-stripped version were generated using a methodology of fMRIPrep 20.2.5 (Esteban et al., 2019, RRID: SCR_016216). A deformation field to correct for susceptibility distortions was estimated based on fMRIPrep's fieldmap-less approach. The deformation field was that resulting from co-registering the BOLD reference to the same-subject T1w-reference with its intensity inverted (Huntenburg, 2014; Wang et al., 2017). Registration was performed with ants Registration (ANTs 2.3.3), and this process was regularized by constraining deformation to be nonzero only along the phase-encoding direction, and modulated with an average fieldmap template (Treiber et al., 2016). Based on the estimated susceptibility distortion, a corrected EPI reference was calculated for a more accurate co-registration with the anatomical reference. The BOLD reference was then co-registered to the T1w reference using bbregister (FreeSurfer), which implemented boundary-based registration (Greve and Fischl, 2009). Co-registration was configured with six degrees of freedom. Head-motion parameters concerning the BOLD reference (transformation matrices and six corresponding rotation and translation parameters) were estimated before any spatiotemporal filtering using mcflirt (FSL 5.0.9; Jenkinson et al., 2002). BOLD runs were slice-time corrected to 0.959 s (0.5 of slice acquisition range 0s-1.92 s) using 3dTshift from AFNI 20,160,207 (Cox and Hyde, 1997, RRID: SCR_005927). The BOLD time-series (including slice-timing correction when applied) were resampled onto their original, native space by applying a single, composite transform to correct for head-motion and susceptibility distortions. These resampled BOLD time-series would be referred to as preprocessed BOLD in original space, or just preprocessed BOLD. The BOLD time-series were resampled into several standard spaces, correspondingly generating the following spatially normalized, preprocessed BOLD runs: MNI152NLin6Asym, MNI152NLin2009cAsym. Several confounding time-series were calculated based on the preprocessed BOLD: FD, DVARS, and three region-wise global signals. FD was computed using two formulations following Power (absolute sum of relative motions; Power et al., 2014) and Jenkinson (relative root mean square displacement between affines, Jenkinson et al., 2002). FD and DVARS were calculated for each functional run, both using their implementations in Nipype (following the definitions by Power et al., 2014). Frames that exceeded a threshold of 0.5 mm FD or 1.5 standardized DVARS were annotated as motion outliers. The three global signals were extracted within the CSF, the WM, and the whole-brain masks. *Re*-samplings were then performed with a single interpolation step by composing all the pertinent transformations (i.e., head-motion transform matrices, susceptibility distortion correction when available, and co-registrations to anatomical and output spaces). Gridded (volumetric) re-samplings were performed using antsApplyTransforms (ANTs), configured with Lanczos interpolation to minimize the smoothing effects of other kernels (Lanczos, 1964).

2.7. Representational similarity analysis

Prior to analysis, the unsmoothed functional data were modeled using the first-level analysis in SPM 12 to obtain single-trial *t*-statistics maps for each participant. We used the least squares single (LSS) approach for single-trial modeling. LSS has been shown to be the most accurate method for decomposing events with different durations and

large signal overlap (Arco et al., 2018). This method allowed a GLM to be constructed individually for each trial, with the trial of interest as one regression term and all other trials as another in the design matrices. The time window of interest was set to the period of the presentation of the recipient's picture. This time window was used for the following reasons: 1) participants had maximized emotional responses, 2) participants might consider how to allocate the amount during this time, and 3) to avoid confusion regarding the activation of prefrontal regions caused by pressing the button. To control for potential head motion and physiological noise, six head motion parameters (i.e., three rotations and three translations), CSF, WM, DVARS, and FD provided by fMRIPrep were included in the design matrices. In addition, all time points with 0.5 mm FD or 1.5 standardized DVARS were censored in the models. All regression terms were convolved with the canonical hemodynamic response function (HRF), and low-frequency drift was removed with a 1/128 Hz high-pass filter. The one-sample *t*-tests were then used to obtain the single-trial *t*-statistics maps.

The RSA was performed in MATLAB R2020a using CoSMoMVPA (http://cosmomvpa.org; Oosterhof et al., 2016, RRID: SCR_014519). The RSA performed here consisted of four steps: 1) building a representational dissimilarity matrix (RDM) of the recipients' emotions; 2) building a neural RDM; 3) searchlight analysis; 4) group-level statistical test. First, the RDM of recipients' emotions was constructed for each participant by setting the value to 0 if two recipients had the same emotion and to 1 if they had different emotions, so that each value in the RDM represented the similarity or dissimilarity of the emotions of the two recipients. Second, the neural RDM was constructed for each participant. For each voxel, a searchlight of 125 voxels centered on that voxel was constructed. The correlation coefficient matrix was generated by extracting the *t*-values of 125 voxels from the single-trial *t*-statistics map of each trial, then calculating the Pearson correlation coefficient (*r*) between the *t*-values of 125 voxels for paired stimulus, followed by 1-*r* to obtain the neural RDM. Third, the searchlight method was used to calculate the representational similarity scores between the RDM of recipients' emotions and the neural RDM (Fig. 1B). For the calculation of representational similarity scores, only the unique off-diagonal values of the matrices were used to compute the Spearman's rank correlation coefficient. The resulting correlation coefficient was then assigned to the voxel at the center of the searchlight. A prior brain mask was employed here to restrict the voxels within brain tissue. This step generated a representational similarity scores image for each participant. To improve the normality of the data, the Fisher Z-transformation was performed on all representational similarity scores images. Higher similarity scores indicate that the brain activity patterns more closely reflect the representations of recipients' emotions, suggesting that the brain region is involved in processing or representing recipients' emotions. Finally, the two-sample *t*-test was used to test for differences between the representational similarity scores images between young and older adults. The significance threshold was set at an uncorrected cluster-forming threshold of $z > 2.3$ and a Gaussian random field (*GRF*) corrected cluster threshold of $p < 0.05$. Besides RSA, we also performed traditional univariate activation analysis that examined the main effect of age, recipients' emotions and their interaction on the brain activity during recipient presentation; see Figure S2 and Table S1 in the Supplementary

Material for results.

2.8. Gray matter volume analysis

The Computational Anatomy Toolbox for SPM (CAT12; http://www.neuro.uni-jena.de/cat, RRID:SCR_019184) was used to process the structural images. During preprocessing, T1-weighted images were corrected for bias-field inhomogeneity, segmented into GM, WM, and CSF (Ashburner and Friston, 2005), and spatially normalized using the DARTEL algorithm (Ashburner, 2007). All scans underwent automated quality assurance using the CAT12 "Check Sample Homogeneity" procedure. None of the images analyzed showed any abnormality. To investigate whether there are structural differences in the different brain regions revealed by the RSA between young and older adults, we extracted the mean GMV of the corresponding brain regions and performed statistical analysis using two-sample *t*-test, and TIV was included as an additional covariate. False discovery rate (*FDR*) was used to control for correction of multiple comparisons.

2.9. The correlation analysis between brain and behavior

Because we hypothesized that the DMPFC integrated social and emotional information to calculate the relative subjective value for self and others, we calculated the partial Pearson correlation coefficients between the representational similarity scores of the left DMPFC and allocations (sad - neutral) in the scanner and between the mean GMV of the left DMPFC and allocations (sad - neutral) in the scanner across age groups. Note that when calculating the correlation between mean GMV of left DMPFC and allocations, in addition to controlling for education, TIV was also included as a covariate. Besides, we also exploratively calculated the partial Pearson correlation coefficients between the representational similarity scores of the left DMPFC and allocations (sad - neutral) outside the scanner and between the mean GMV of the left DMPFC and allocations (sad - neutral) outside the scanner across age groups.

2.10. Mediation analysis

To test whether and how age influences allocations via the function and structure of related brain regions, we conducted two serial mediation analyses using the R package lavaan (https://cran.r-project.org/web/packages/lavaan/index.html; Rosseel, 2012). In the first model, we considered age (dummy variable; young adults were coded "−1″ and older adults were coded "1″) as the independent variable, participants' allocations (sad-neutral) in the scanner as the dependent variable, representational similarity scores (i.e., Fisher Z-transformed Spearman's rank correlation coefficients) of the right insula and left DMPFC as mediator variables, with education as a covariate; in the second model, however, the mean GMV of the right ACC and left DMPFC were considered as the mediator variables, with education and TIV as covariates. The nonparametric bootstrap approach with 5000 iterations estimated the indirect and direct effects at a 95 % bias-corrected percentile. The standardized regression coefficients and 95 % confidence intervals (CI) were reported. Indirect and direct effects were considered statistically significant if their 95 % CI did not include zero. In addition to testing the above models, we performed supplementary analyses using the representational similarity scores of the right ACC and the left DPMFC or the mean GMV of the right insula and the left DMPFC as mediator variables; see Supplementary Material (Figure S3) for results.

3. Results

3.1. Behavioral results

The allocations in the scanner showed a significant interaction of age × recipients' emotions ($F_{(1,60)} = 4.30$, $p = 0.04$, $\eta_p^2 = 0.07$; Fig. 2A). The subsequent simple effect analysis revealed that young adults allocated more amounts to sad recipients than that to neutral recipients ($t_{(60)} = 2.29$, $p = 0.03$, *Cohen's d* = 0.53), whereas there was no significant difference between sad and neutral recipients in older adults ($t_{(60)} = -1.14$, $p = 0.26$, *Cohen's d* = −0.26). Besides, there was no significant difference in the allocations between young and older adults for neutral recipients ($t_{(60)} = 1.03$, $p = 0.31$, *Cohen's d* = 0.53), but young adults allocated more amounts than older adults for sad recipients ($t_{(60)} = 2.49$, $p = 0.02$, *Cohen's d* = 1.32), as revealed by another type of simple effects analysis. Thus, older adults' allocations in the scanner showed a

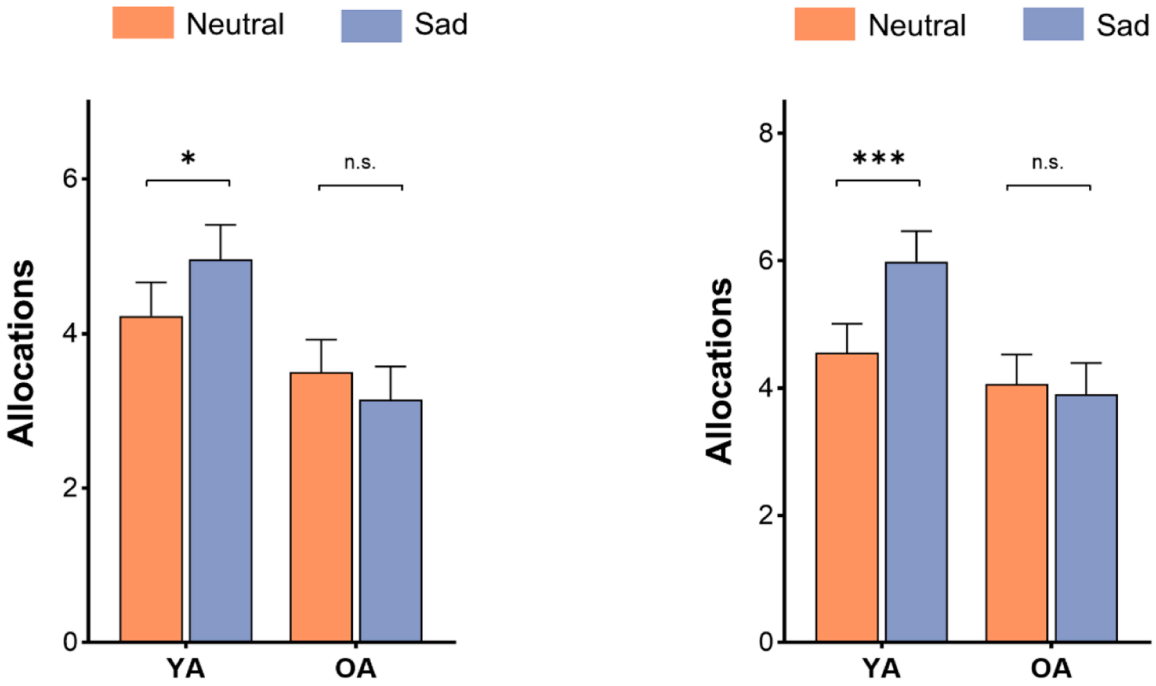

Fig. 2. The behavioral allocation results (A) in the scanner and (B) outside the scanner. * $p < 0.05$; ** $p < 0.01$; *** $p < 0.001$; *n.s.* represents no significance. YA, young adults; OA, older adults. The error bar indicates the ± 1 standardized error of estimated marginal means.

decrease in emotion-related generosity compared to young adults. The main effects of age ($F_{(1,60)} = 3.61$, $p = 0.06$, $\eta_p^2 = 0.06$) and recipients' emotions ($F_{(1,60)} = 1.13$, $p = 0.29$, $\eta_p^2 = 0.02$) were not significant.

The results of the allocation questionnaire completed outside the scanner were similar to the allocations in the scanner, which showed a significant interaction of age × recipients' emotions ($F_{(1,58)} = 7.21$, $p = 0.009$, $\eta_p^2 = 0.11$; Fig. 2B). The subsequent simple effects analysis revealed that young adults allocated more amounts to sad recipients than that to neutral recipients ($t_{(58)} = 4.04$, $p < 0.001$, *Cohen's d* = 0.92), whereas there was no significant difference between sad and neutral recipients in older adults ($t_{(58)} = -0.44$, $p = 0.66$, *Cohen's d* = −0.10). Furthermore, another type of simple effects analysis showed there was no significant difference in the allocations between young and older adults for neutral recipients ($t_{(58)} = 0.65$, $p = 0.52$, *Cohen's d* = 0.32), but young adults allocated more amounts than older adults for sad recipients ($t_{(58)} = 2.59$, $p = 0.01$, *Cohen's d* = 1.34).Therefore, older adults' allocations outside the scanner also showed a decrease in emotion-related generosity compared to young adults. The main effect of age ($F_{(1,58)} = 3.17$, $p = 0.08$, $\eta_p^2 = 0.05$) was not significant, whereas the main effect of recipients' emotions was significant ($F_{(1,58)} = 10.77$, $p = 0.002$, $\eta_p^2 = 0.16$), with the amounts allocated to sad recipients higher than that to neutral recipients ($t_{(58)} = 3.14$, $p = 0.003$, *Cohen's d* = 0.41).

Moreover, we also conducted the control analyses. The 2 (age) × 2 (recipients' ages) × 2 (recipients' emotions) repeated measures ANCOVAs were used to examine the moderating effect of recipients' ages on participants' allocations. The results showed that the recipients' ages did not have the significant moderating effects on allocations both in the scanner and outside the scanner (Table S2).

3.2. Age differences in neural representations of recipients' emotions

The representational similarity analysis revealed that young adults had higher representational similarity scores than older adults in the left caudate, left DMPFC, right insula and right ACC, but older adults had higher representational similarity scores than young adults in the right angular gyrus (Table 2; Fig. 3). After additionally controlling for univariate activation in related brain regions, the above results remained consistent (Table S3). We also controlled the mean GMV to reanalyze the differences in representational similarity scores between young and older adults. The results showed that there was no significant difference in representational similarity scores of the right insula and right angular gyrus between young and older adults after controlling for mean GMV, while the results of other brain regions remained consistent (Table S3), suggesting that the age differences in representational similarity scores of the right insula and right angular gyrus might be related to the declines in gray matter volume in older adults. Moreover, to control for the

Table 2
The results of representational similarity analysis of recipients' emotions.

Regions	L/R	BA	MNI coordinates			*Z*	Voxels
			x	y	z		
YA > OA							
Caudate	L	–	−22	2	18	4.59	144
Dorsomedial prefrontal cortex	L	32	−10	26	34	4.05	125
Anterior cingulate gyrus	R	24	6	34	14	4.05	136
Insula	R	48	34	18	4	3.70	112
OA > YA							
Angular gyrus	R	39 40	−54	44		4.12	123

Note. The significance threshold was set at an uncorrected cluster-forming threshold of $z > 2.3$ and a *GRF* corrected cluster threshold of $p < 0.05$. L, the left hemisphere; R, the right hemisphere; BA, Brodmann area; YA, young adults; OA, older adults.

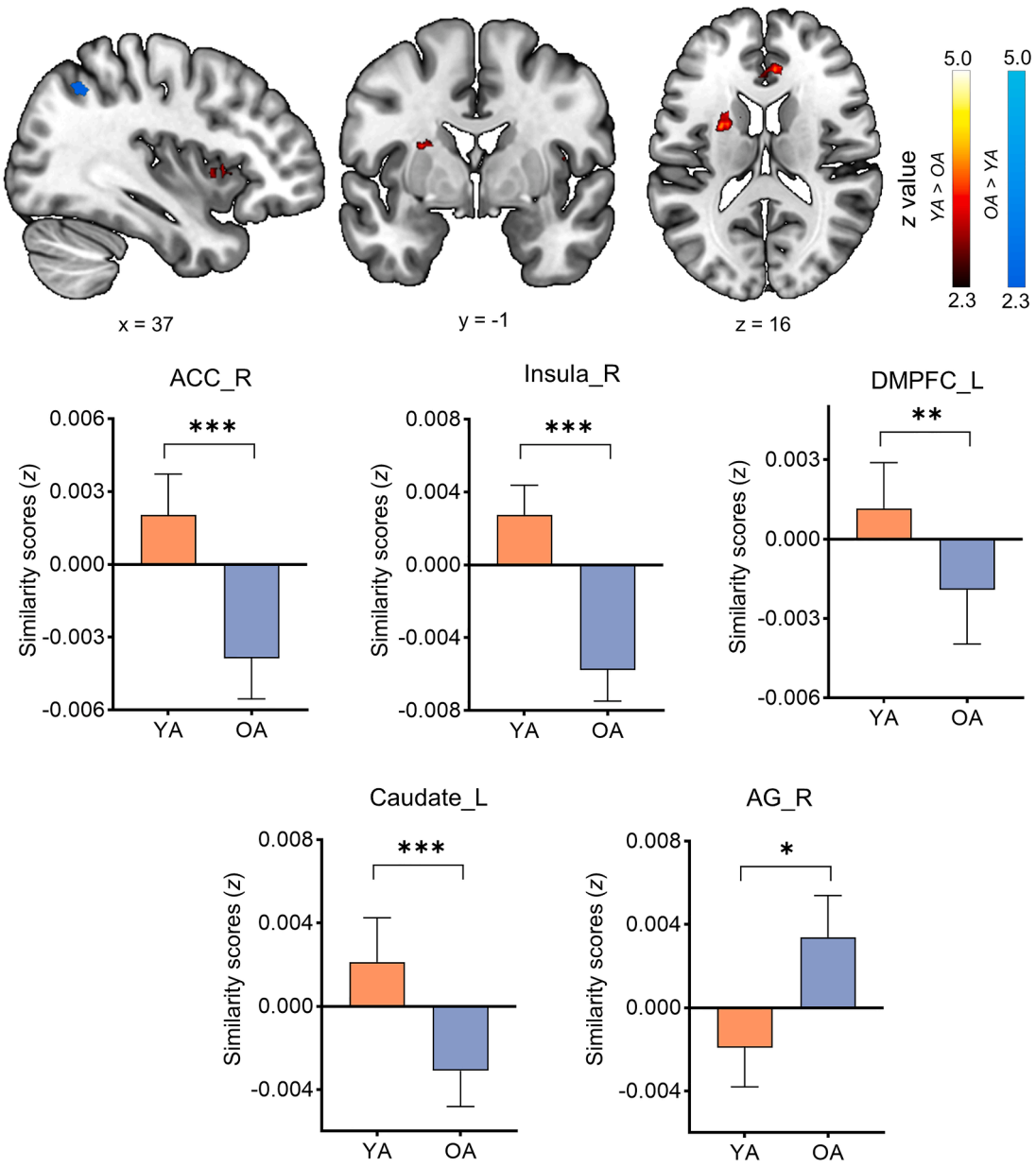

Fig. 3. Brain regions that differ in representational similarity scores between young and older adults. The significance threshold was set at an uncorrected cluster-forming threshold of $z > 2.3$ and a GRF corrected cluster threshold of $p < 0.05$. * $p < 0.05$; ** $p < 0.01$; *** $p < 0.001$; ACC, anterior cingulate gyrus; DMPFC, dorsomedial prefrontal cortex; YA, young adults; OA, older adults; L, left hemisphere; R, right hemisphere. The error bar indicates the ± 1 standardized error of means (SEM). All *p*-values are *FDR* corrected.

effects of recipients' ages, we additionally constructed the RDM of recipients' ages in the representational similarity analysis by setting the value to 0 if two recipients were the same age and to 1 if they were different ages. When calculating the representational similarity scores between the neural RDM and the RDM of recipients' emotions, the partial Spearman's rank correlation was performed with the RDM of recipients' ages as a covariate. The results remained highly consistent (Table S4; Figure S4).

3.3. Age differences in gray matter volume

The results revealed that young adults had higher mean GMV than older adults in the right ACC, right insula, left DMPFC, left caudate, and right angular gyrus (Fig. 4).

3.4. The correlation between brain and behavior

The correlation analyses found the representational similarity scores of the left DMPFC were positively related to the allocations in the scanner across age groups ($r = 0.34$, $p = 0.006$; Fig. 5A), and the mean GMV of the left DMPFC was positively related to the allocations in the scanner across age groups ($r = 0.32$, $p = 0.01$; Fig. 5B). Exploratory correlation analyses also revealed the representational similarity scores of the left DMPFC were positively related to the allocations outside the scanner across age groups ($r = 0.33$, $p = 0.01$; Figure S5A), and the mean GMV of the left DMPFC was positively related to the allocations outside the scanner across age groups ($r = 0.37$, $p = 0.003$; Figure S5B).

3.5. The results of serial mediation analysis

The bootstrap tests were used to test whether the direct and indirect

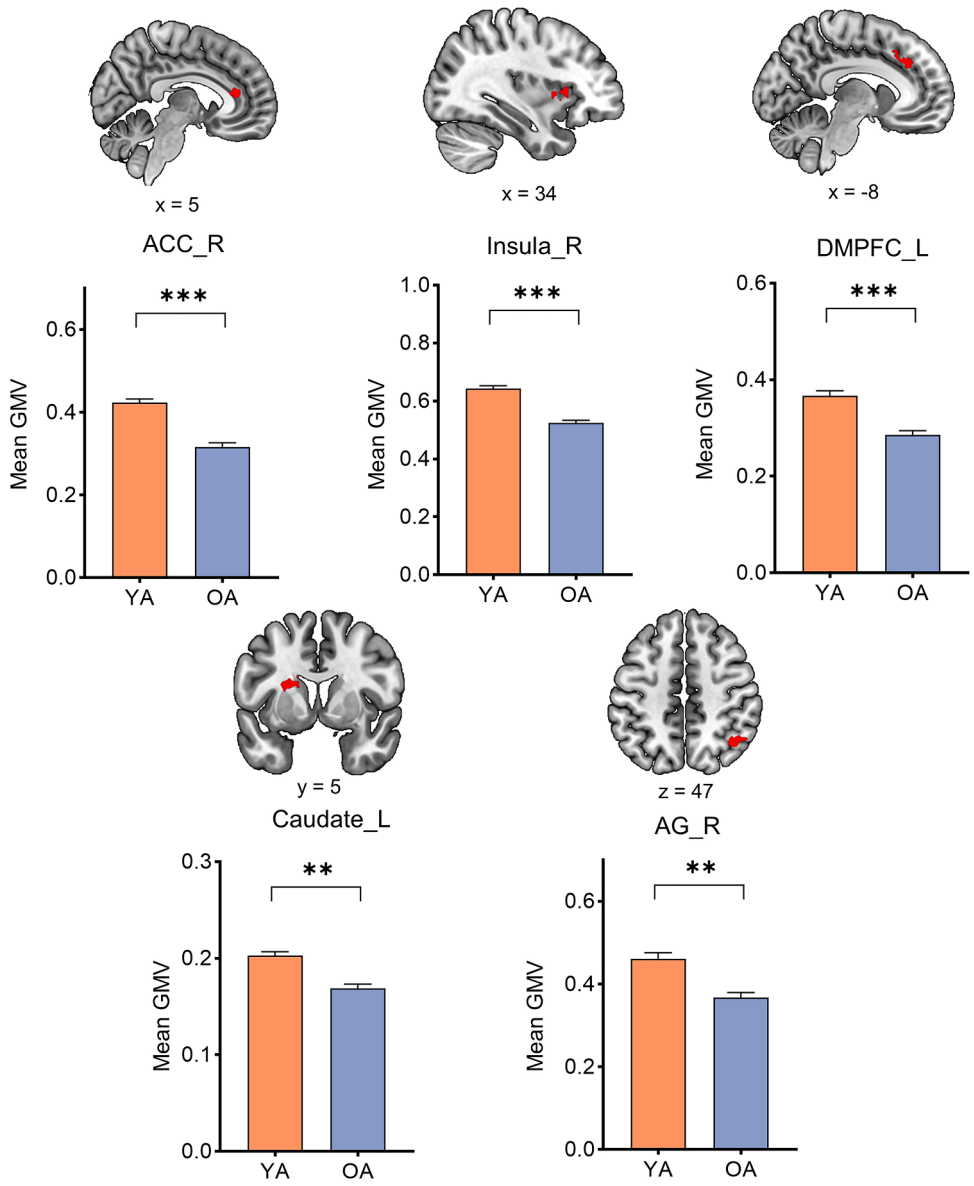

Fig. 4. Brain regions that differ in mean GMV between young and older adults. The significance threshold was set at an uncorrected cluster-forming threshold of $z > 2.3$ and a GRF corrected cluster threshold of $p < 0.05$. * $p < 0.05$; ** $p < 0.01$; *** $p < 0.001$; ACC, anterior cingulate gyrus; DMPFC, dorsomedial prefrontal cortex; L, left hemisphere; R, right hemisphere; GMV, gray matter volume; YA, young adults; OA, older adults. The error bar indicates the ±1 SEM. All *p*-values are *FDR* corrected.

effects of age on allocations in the scanner were significant. The first model yielded a significant serial mediation effect via the representational similarity scores of the right insula and left DMPFC ($\beta_3 = -0.06$, 95 % CI = [−0.17, −0.01]). The indirect effect via the representational similarity scores of the left DMPFC was also significant ($\beta_2 = -0.08$, 95 % CI = [−0.22, −0.01]), but the indirect effect via the representational similarity scores of the right insula ($\beta_1 = -0.07$, 95 % CI = [−0.24, 0.09]) and the direct effect of age on allocations ($\beta = -0.17$, 95 % CI = [−0.56, 0.25]) were not significant (Fig. 5C). The second model also showed a significant serial mediation effect via the mean GMV of the right ACC and left DMPFC ($\beta_3 = -0.09$, 95 % CI = [−0.26, −0.02]). Besides, the indirect effect via the mean GMV of the left DMPFC was also significant ($\beta_2 = -0.17$, 95 % CI = [−0.44, −0.04]), but the indirect effect via the mean GMV of the right ACC ($\beta_1 = 0.15$, 95 % CI = [−0.17, 0.50]) and the direct effect of age on allocations ($\beta = -0.26$, 95 % CI = [−0.78, 0.31]) were not significant (Fig. 5D).

Besides, we performed the exploratory mediation analyses using the allocations outside the scanner as the dependent variable. Except for the non-significant path coefficient via the representation similarity scores of the left DMPFC to allocations, other indirect effect paths were consistent with the results of the allocations in the scanner as the dependent variable (Figure S5C; Figure S5D). We speculated that the reason for the non-significant path coefficient via the representation similarity analysis scores of the left DMPFC to allocations was likely due to the non-simultaneity between the neural activity in the scanner and the behavioral measures outside the scanner, which weakened the brain-behavior correlation.

4. Discussion

This study used the dictator game task to examine differences in monetary allocations between young and older adults in response to recipients with different facial emotions. Behavioral results revealed that older adults' allocations showed a decrease in emotion-related generosity compared to young adults. Neurally, the representational similarity scores in the right insula, right ACC, left DMPFC, and left

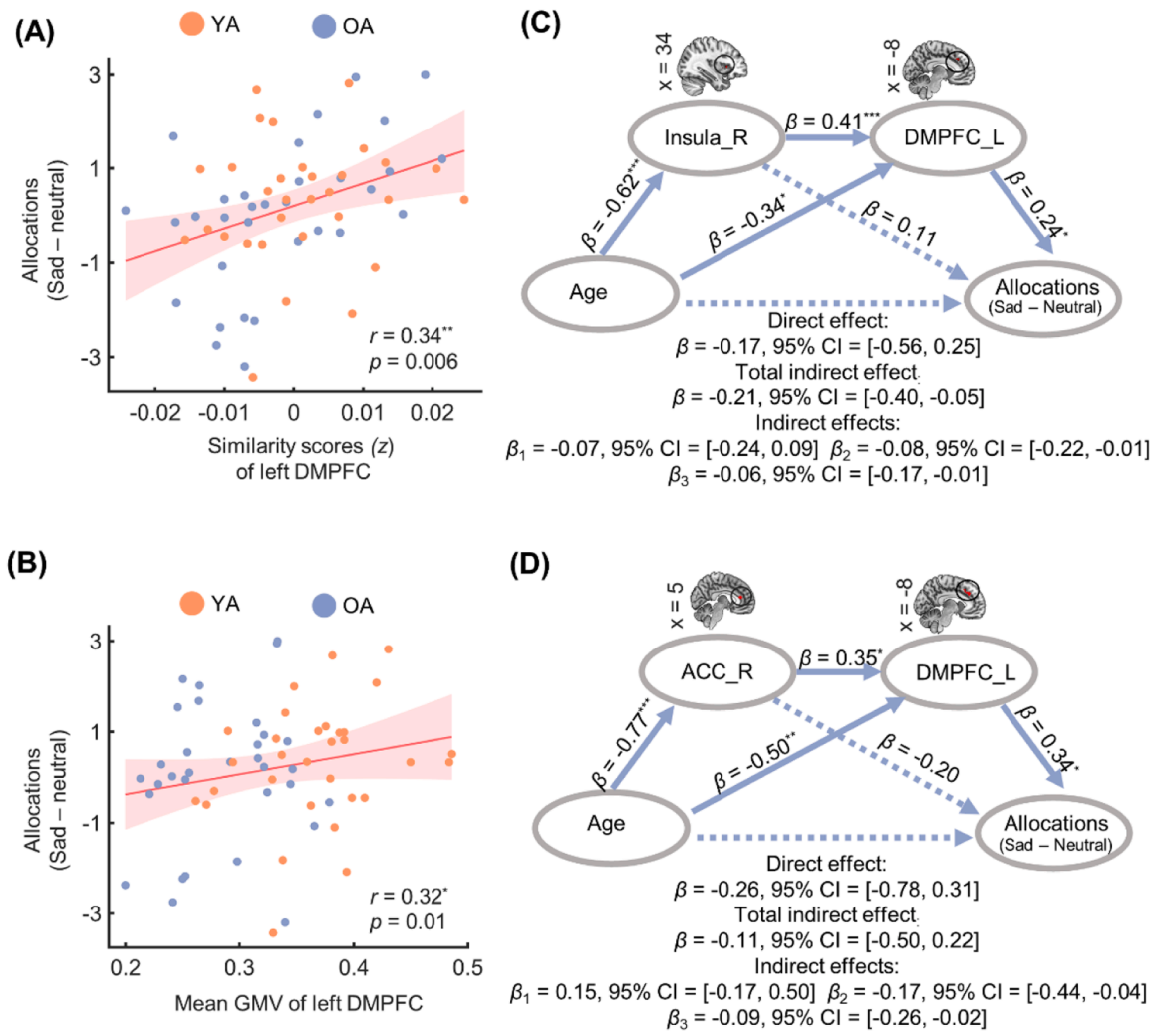

Fig. 5. . (A) The correlation between the representational similarity scores of the left DMPFC and allocations in the scanner. (B) The correlation between the mean GMV of the left DMPFC and allocations in the scanner. (C) The results of the serial mediation analysis with the representational similarity scores of the right insula and left DMPFC as the mediator variables and allocations in the scanner as the dependent variable. β_1 indicates the path from age via the representational similarity scores of the right insula to allocations; β_2 indicates the path from age via the representational similarity scores of the left DMPFC to allocations; β_3 indicates the path from age via the representational similarity scores of the right insula and left DMPFC to allocations. (D) The results of the serial mediation analysis with the mean GMV of the right ACC and left DMPFC as the mediator variables and allocations in the scanner as the dependent variable. β_1 indicates the path from age via the mean GMV of the right ACC to allocations; β_2 indicates the path from age via the mean GMV of the left DMPFC to allocations; β_3 indicates the path from age via the mean GMV of the right ACC and left DMPFC to allocations. GMV, gray matter volume; CI, confidence interval; ACC, anterior cingulate gyrus; DMPFC, dorsomedial prefrontal cortex; L, left hemisphere; R, right hemisphere; *$p < 0.05$; ** $p < 0.01$; ***$p < 0.001$; YA, young adults; OA, older adults.

caudate were higher in young adults than in older adults, but the representational similarity scores in the right angular gyrus were higher in older adults than in young adults. Besides, the mean GMV in the right insula, right ACC, the left DMPFC, left caudate and the right angular gyrus were higher in young adults than in older adults. Importantly, the representational similarity scores between the right insula and the left DMPFC and the mean GMV between the right ACC and the left DMPFC played significant serial mediation roles between age and allocations.

Compared to young adults, older adults' allocations showed a decrease in emotion-related generosity. First, we speculated that it might be related to older adults' decreased ability to process sad facial expressions (Gonçalves et al., 2018; MacPherson et al., 2006). Older adults' positive emotion bias in emotion processing (Carstensen, 1992, 2021; Carstensen et al., 1999; Moore et al., 2015) and related cognitive declines (Lambrecht et al., 2012) impair their ability to process negative emotions, which in turn impact older adults' ability to understand the motives and intentions of others in social decision making, ultimately resulting in changes in older adults' allocation behavior. Second, it may also be due to the decline in their ability to integrate emotions (Baena et al., 2010; Charles and Carstensen, 2010), making it difficult for older adults to integrate information from recipients with different emotions to guide allocation behavior. In sum, although our findings suggested differences in emotion-related generosity between older and young adults, there was no evidence that older adults were less generous than young adults overall. Therefore, our results proved that older adults were not less generous unless confronted with individuals with specific emotions (such as sad). Besides, the decrease in emotion-related generosity in older adults cannot be explained by differences in empathy, as no differences were found on any of the dimensions of the IRI-C scale (Table 1), and was more likely related to altered emotion processing and integration abilities in older adults.

The neuroimaging results showed that the representational similarity scores and mean GMV of the right insula and right ACC were significantly higher in young adults than in older adults. The ACC and insula, as key nodes of the salience network/midcingulo-insular network (Menon and Uddin, 2010; Toga, 2015; Ziaei et al., 2021), are closely

linked to emotion processing, and their function and structure are particularly vulnerable to aging. For instance, when viewing scenarios of others' body parts being injured, older adults had reduced activation of the insula and ACC compared to young adults (Chen et al., 2014). A recent study had also found that emotional reactivity declines with age and that the GMV of the insula was negatively correlated with age (Niu et al., 2024). Interestingly, resting-state functional connectivity (RSFC) of the left insula with the right hippocampus and the RSFC of the right insula with the striatum and thalamus mediated the relationship between age and emotional reactivity (Niu et al., 2024). Besides, there has been evidence of an association between reduced insula activity and disturbances in emotional processing in clinical conditions such as neurodegenerative diseases (Verstaen et al., 2016), Parkinson's disease (Vicario et al., 2017), and stroke (Vicario et al., 2017), which typically occur in aging populations. Thus, the structural and functional changes in the right ACC and right insula in older adults may reduce their processing of others' emotions and their ability to understand and respond to the emotional states of others (Chen et al., 2014; Mather, 2012, 2016; Orlando and Filippini, 2024; Ziaei et al., 2021). These findings were consistent with previous behavioral studies that older adults have more difficulty to process negative emotions than positive emotions compared to young adults (Hayes et al., 2020; Ruffman et al., 2008), and provided partial neural evidence for socioemotional selectivity theory, which proposes that older adults preferentially process positive over negative stimuli (Carstensen, 1992, 2021; Carstensen et al., 1999).

We also found that the representational similarity scores and mean GMV of the left DMPFC were significantly lower in older adults than in young adults. The DMPFC is involved in integrating social and emotional information (Ding et al., 2020; Krishnan et al., 2016; Wever et al., 2021). Hence, the reduced neural representations and structural integrity in older adults may also be related to the decline in the integration of social and emotional information. Moreover, our results also showed that both representational similarity scores and mean GMV of the left DMPFC were positively correlated with allocations across age groups, suggesting that the left DMPFC might influence allocations by integrating social and emotional information to compute the relative subjective value for self and others (Ferrari et al., 2016; Kensinger and Ford, 2021; Martin et al., 2017; Piva et al., 2019; Tomova et al., 2020). Therefore, the functional and structural deficits in the left DMPFC in older adults might impact how older adults integrated social and emotional information to compute relative subjective value for self and others. This provided a partial neural explanation for older adults' allocations showing a decrease in emotion-related generosity.

Importantly, we found that age influenced allocations not only through serial mediation of the representational similarity scores of the right insula and left DMPFC, but also through serial mediation of the mean GMV of the right ACC and left DMPFC. Specifically, with increasing age, the neural representations of the right insula and the structural integrity of the right ACC decreased in older adults, whereas the neural representations and the structural integrity of the left DMPFC were positively related the neural representations of the right insula and the structural integrity of the right ACC, respectively, ultimately explaining the difference in allocations between young and older adults. These serial relationships might suggest that the impaired the ability to process emotions due to declines in the neural representations of the right insula or the structural integrity of the right ACC did not alone cause decreased emotion-related generosity in older adults. Instead, the ability to integrate emotions processed by the right insula and right ACC to compute the relative subjective value for self and others was also altered as a result of declines in neural representations and structural integrity of the left DMPFC, which further influenced emotion-related generosity in older adults. Moreover, age could also influence allocations through neural representations or structural integrity of the left DMPFC, further supporting the critical role of the left DMPFC in explaining altered emotion-related social decision making in older adults. These potential neural pathways highlighted the complex interactions between emotions and social interactions in the formation of age-related allocation differences, reveal at the neural level that older adults were not less generous unless confronted with individuals with specific emotions (such as sad), and deepen our understanding of their social interaction behavior.

Besides, our results also found that the representational similarity scores and mean GMV of the left caudate were significantly lower in older adults than in young adults. The caudate is a key striatal region, and age-related alterations in the left caudate may affect learning, motivation, and reward processing in older adults (Bick et al., 2019; Fareri et al., 2008; Grahn et al., 2008; Haruno and Kawato, 2006). Interestingly, although older adults showed significantly lower mean GMV of the right angular gyrus compared to young adults, the representational similarity scores of right angular gyrus in older adults were significantly higher than in young adults. The right angular gyrus is strongly linked to processes that require intentional attribution and temporary inferences (Bravo et al., 2017). The reversal of structural and functional differences in the right angular gyrus between young and older adults may reflect changes of related cognitive functions in older adults.

This study examined the effects of changes in function and structure of the ACC, insula, and DMPFC in older adults on emotion-related social decision making and revealed potential neural pathways. However, this study has several limitations. First, there was a significant difference in education between young and older adults. Although this was controlled for as a covariate in all analyses, its influence on the results cannot be ruled out. Future studies should rigorously control for education in both the young and older adults to rule out the effect of education on age-related differences in social decision making. Second, this study only considered neutral and sad recipients. Due to the complexity and diversity of people's emotions, this study cannot fully reveal how other people's emotions affect social decision making in older adults. Future studies should include a greater variety of emotions in their experiments to fully explore age differences in emotion-related social decision making. Third, this study used a dictator game task based on laboratory research to examine social decision making, which may lack ecological validity. Therefore, caution should be exercised in generalizing the results of this study to practical applications. Future research could consider the use of other experimental social decision tasks to further investigate age differences in emotion-related social decision making. In addition, hyperscanning techniques have been increasingly used in recent years to investigate the neural basis of interpersonal social interactions (Ishihara et al., 2024; Liu et al., 2024; Song et al., 2024; Zhang et al., 2024; Zhao et al., 2024). Hyperscanning allows for the simultaneous consideration of interactions in neural activity between multiple participants and enhances ecological validity by allowing the study of real-world behaviors and experiences (Babiloni and Astolfi, 2014; Xie et al., 2020). Therefore, future studies could consider using hyperscanning to investigate the neural basis of age differences in emotion-related social decision making. Finally, the present study revealed the potential neural pathways that explain differences in emotion-related social decision making through serial mediation analyses. However, these neural pathways were currently only the results of mathematical model inference and did not allow for the direct tests of causality. Future studies could consider using neuromodulation techniques to intervene directly in the brain regions to validate the causal relationship.

5. Conclusions

In conclusion, the present study indicated that aging weakened the regulatory effect of others' emotions on social decision making from behavioral and neural perspectives in older adults. Behavior results indicated older adults showed a decline in emotion-related generosity. Neuroimaging results showed functional and structural deficits in the right ACC, right insula, and left DMPFC in older adults compared to

young adults. More importantly, age influenced allocations not only through serial mediation of neural representations of the right insula and left DMPFC, but also through serial mediation of the mean gray matter volume of the right ACC and left DMPFC, which provides potential neural pathways to explain age differences in emotion-related social decision making, advancing our understanding of older adults' social interaction behavior that they may not be less generous unless confronted with individuals with specific emotions.

CRediT authorship contribution statement

Hong-Zhou Xu: Writing – review & editing, Writing – original draft, Visualization, Validation, Software, Methodology, Investigation, Formal analysis, Data curation, Conceptualization. **Xue-Rui Peng:** Writing – review & editing. **Shen-Yin Huan:** Investigation, Data curation. **Jia-Jie Xu:** Investigation, Data curation. **Jing Yu:** Writing – review & editing, Supervision, Project administration, Funding acquisition, Conceptualization. **Qing-Guo Ma:** Writing – review & editing, Funding acquisition.

Declaration of competing interest

The authors declare no conflict of interest.

Data availability

All the processed data and analysis scripts are available on https://osf.io/782z3/. The unthresholded statistical images of representational similarity analysis are available at https://identifiers.org/neurovault.collection:17589.

Ethics statement

All participants provided written informed consent prior to the experiment, and the experimental procedures were approved by the Ethics Committee of Southwest University to be in accordance with the Declaration of Helsinki (H17014).

Funding

This work was supported by the National Natural Science Foundation of China (71942004, 61961160705, and 32371109).

Supplementary materials

Supplementary material associated with this article can be found, in the online version, at doi:10.1016/j.neuroimage.2024.120756.

References

Adolfi, F., Couto, B., Richter, F., Decety, J., Lopez, J., Sigman, M., Manes, F., Ibáñez, A., 2017. Convergence of interoception, emotion, and social cognition: a twofold fMRI meta-analysis and lesion approach. Cortex 88, 124–142.
Allard, E.S., Kensinger, E.A., 2014. Age-related differences in functional connectivity during cognitive emotion regulation. J. Gerontol. Ser. B: Psychol. Sci. Soc. Sci. 69 (6), 852–860.
Apps, M.A., Rushworth, M.F., Chang, S.W., 2016. The anterior cingulate gyrus and social cognition: tracking the motivation of others. Neuron 90 (4), 692–707.
Arco, J.E., González-García, C., Díaz-Gutiérrez, P., Ramírez, J., Ruz, M., 2018. Influence of activation pattern estimates and statistical significance tests in fMRI decoding analysis. J. Neurosci. Methods 308, 248–260.
Ashburner, J., 2007. A fast diffeomorphic image registration algorithm. Neuroimage 38 (1), 95–113.
Ashburner, J., Friston, K.J., 2005. Unified segmentation. Neuroimage 26 (3), 839–851.
Avants, B.B., Epstein, C.L., Grossman, M., Gee, J.C., 2008. Symmetric diffeomorphic image registration with cross-correlation: evaluating automated labeling of elderly and neurodegenerative brain. Med. Image Anal. 12 (1), 26–41.
Babiloni, F., Astolfi, L., 2014. Social neuroscience and hyperscanning techniques: past, present and future. Neurosci. Biobehav. Rev. 44, 76–93.
Baena, E., Allen, P.A., Kaut, K.P., Hall, R.J., 2010. On age differences in prefrontal function: the importance of emotional/cognitive integration. Neuropsychologia 48 (1), 319–333.
Bick, S.K., Patel, S.R., Katnani, H.A., Peled, N., Widge, A., Cash, S.S., Eskandar, E.N., 2019. Caudate stimulation enhances learning. Brain 142 (10), 2930–2937.
Bravo, F., Cross, I., Hawkins, S., Gonzalez, N., Docampo, J., Bruno, C., Stamatakis, E.A., 2017. Neural mechanisms underlying valence inferences to sound: the role of the right angular gyrus. Neuropsychologia 102, 144–162.
Brocklebank, S., Lewis, G.J., Bates, T.C., 2011. Personality accounts for stable preferences and expectations across a range of simple games. Pers. Individ. Dif. 51 (8), 881–886.
Bruneau, E.G., Pluta, A., Saxe, R., 2012. Distinct roles of the 'shared pain' and 'theory of mind' networks in processing others' emotional suffering. Neuropsychologia 50 (2), 219–231.
Carstensen, L.L., 1992. Social and emotional patterns in adulthood: support for socioemotional selectivity theory. Psychol. Aging 7 (3), 331.
Carstensen, L.L., 2021. Socioemotional selectivity theory: the role of perceived endings in human motivation. Gerontologist 61 (8), 1188–1196.
Carstensen, L.L., Isaacowitz, D.M., Charles, S.T., 1999. Taking time seriously: a theory of socioemotional selectivity. Am. Psychol. 54 (3), 165.
Cassidy, B.S., Leshikar, E.D., Shih, J.Y., Aizenman, A., Gutchess, A.H., 2013. Valence-based age differences in medial prefrontal activity during impression formation. Soc. Neurosci. 8 (5), 462–473.
Charles, S.T., Carstensen, L.L., 2010. Social and emotional aging. Annu. Rev. Psychol. 61, 383–409.
Charness, G., Rabin, M., 2002. Understanding social preferences with simple tests. Quart. J. Econ. 117 (3), 817–869.
Chen, Y.-C., Chen, C.-C., Decety, J., Cheng, Y., 2014. Aging is associated with changes in the neural circuits underlying empathy. Neurobiol. Aging 35 (4), 827–836.
Cox, R.W., Hyde, J.S., 1997. Software tools for analysis and visualization of fMRI data. NMR in Biomed.: Int. J. Devoted Develop. Appl. Mag. Resonance In Vivo 10 (4–5), 171–178.
Dimsdale-Zucker, H.R., Ranganath, C., 2018. Representational similarity analyses: a practical guide for functional MRI applications. In: Handbook of Behavioral Neuroscience, 28. Elsevier, pp. 509–525.
Ding, R., Ren, J., Li, S., Zhu, X., Zhang, K., Luo, W., 2020. Domain-general and domain-preferential neural correlates underlying empathy towards physical pain, emotional situation and emotional faces: an ALE meta-analysis. Neuropsychologia 137, 107286.
Dobrushina, O.R., Arina, G.A., Dobrynina, L.A., Suslina, A.D., Solodchik, P.O., Belopasova, A.V., Gubanova, M.V., Sergeeva, A.N., Kremneva, E.I., Krotenkova, M. V., 2020. The ability to understand emotions is associated with interoception-related insular activation and white matter integrity during aging. Psychophysiology 57 (5), e13537.
Esteban, O., Markiewicz, C.J., Blair, R.W., Moodie, C.A., Isik, A.I., Erramuzpe, A., Kent, J. D., Goncalves, M., DuPre, E., Snyder, M., 2019. fMRIPrep: a robust preprocessing pipeline for functional MRI. Nat. Methods 16 (1), 111–116.
Fareri, D.S., Martin, L.N., Delgado, M.R., 2008. Reward-related processing in the human brain: developmental considerations. Dev. Psychopathol. 20 (4), 1191–1211.
Ferrari, C., Lega, C., Vernice, M., Tamietto, M., Mende-Siedlecki, P., Vecchi, T., Todorov, A., Cattaneo, Z., 2016. The dorsomedial prefrontal cortex plays a causal role in integrating social impressions from faces and verbal descriptions. Cereb. Cort. 26 (1), 156–165.
Fratiglioni, L., Paillard-Borg, S., Winblad, B., 2004. An active and socially integrated lifestyle in late life might protect against dementia. Lancet Neurol. 3 (6), 343–353.
Frazier, I., Lighthall, N.R., Horta, M., Perez, E., Ebner, N.C., 2019. CISDA: changes in integration for social decisions in aging. Wiley Interdiscipl. Rev.: Cogn. Sci. 10 (3), e1490.
Gonçalves, A.R., Fernandes, C., Pasion, R., Ferreira-Santos, F., Barbosa, F., Marques-Teixeira, J., 2018. Effects of age on the identification of emotions in facial expressions: a meta-analysis. PeerJ 6, e5278.
Gong, X., Huang, Y.-X., Wang, Y., & Luo, Y.-J. (2011). Revision of the Chinese facial affective picture system. *Chin. Mental Health J.*.
Grahn, J.A., Parkinson, J.A., Owen, A.M., 2008. The cognitive functions of the caudate nucleus. Prog. Neurobiol. 86 (3), 141–155.
Greve, D.N., Fischl, B., 2009. Accurate and robust brain image alignment using boundary-based registration. Neuroimage 48 (1), 63–72.
Gunning-Dixon, F.M., Gur, R.C., Perkins, A.C., Schroeder, L., Turner, T., Turetsky, B.I., Chan, R.M., Loughead, J.W., Alsop, D.C., Maldjian, J., 2003. Age-related differences in brain activation during emotional face processing. Neurobiol. Aging 24 (2), 285–295.
Haruno, M., Kawato, M., 2006. Different neural correlates of reward expectation and reward expectation error in the putamen and caudate nucleus during stimulus-action-reward association learning. J. Neurophysiol. 95 (2), 948–959.
Hayes, G.S., McLennan, S.N., Henry, J.D., Phillips, L.H., Terrett, G., Rendell, P.G., Pelly, R.M., Labuschagne, I., 2020. Task characteristics influence facial emotion recognition age-effects: a meta-analytic review. Psychol. Aging 35 (2), 295.
Hettich, D., Hattula, S., Bornemann, T., 2018. Consumer decision-making of older people: a 45-year review. Gerontologist 58 (6), e349–e368.
Huntenburg, J.M., 2014. *Evaluating Nonlinear Coregistration of BOLD EPI and T1w Images* Freie. Universität Berlin.].
Ishihara, T., Hashimoto, S., Tamba, N., Hyodo, K., Matsuda, T., Takagishi, H., 2024. The links between physical activity and prosocial behavior: an fNIRS hyperscanning study. Cereb. Cort. 34 (2), bhad509.
Izuma, K., Adolphs, R., 2013. Social manipulation of preference in the human brain. Neuron 78 (3), 563–573.
Jenkinson, M., Bannister, P., Brady, M., Smith, S., 2002. Improved optimization for the robust and accurate linear registration and motion correction of brain images. Neuroimage 17 (2), 825–841.

Jobson, D.D., Hase, Y., Clarkson, A.N., Kalaria, R.N., 2021. The role of the medial prefrontal cortex in cognition, ageing and dementia. Brain Commun. 3 (3), fcab125.
Kanel, D., Al-Wasity, S., Stefanov, K., Pollick, F.E., 2019. Empathy to emotional voices and the use of real-time fMRI to enhance activation of the anterior insula. Neuroimage 198, 53–62.
Kensinger, E.A., Ford, J.H., 2021. Guiding the emotion in emotional memories: the role of the dorsomedial prefrontal cortex. Curr. Dir. Psychol. Sci. 30 (2), 111–119. https://doi.org/10.1177/0963721421990081.
Krishnan, A., Woo, C.-W., Chang, L.J., Ruzic, L., Gu, X., López-Solà, M., Jackson, P.L., Pujol, J., Fan, J., Wager, T.D., 2016. Somatic and vicarious pain are represented by dissociable multivariate brain patterns. Elife 5, e15166.
Lambrecht, L., Kreifelts, B., Wildgruber, D., 2012. Age-related decrease in recognition of emotional facial and prosodic expressions. Emotion 12 (3), 529.
Lanczos, C., 1964. Evaluation of noisy data. J. Soc. Ind. Appl. Mathe. Ser. B: Numer. Anal. 1 (1), 76–85.
Leclerc, C.M., Kensinger, E.A., 2008. Age-related differences in medial prefrontal activation in response to emotional images. Cogn. Affec. Behav. Neurosci. 8, 153–164.
Levine, S.M., Schwarzbach, J.V., 2021. Individualizing representational similarity analysis. Front. Psychiatry 12, 729457.
Liu, Q., Cui, H., Huang, B., Huang, Y., Sun, H., Ru, X., Zhang, M., Chen, W., 2024. Inter-brain neural mechanism and influencing factors underlying different cooperative behaviors: a hyperscanning study. Brain Struc. Func. 229 (1), 75–95.
Lockwood, P.L., Abdurahman, A., Gabay, A.S., Drew, D., Tamm, M., Husain, M., Apps, M. A., 2021. Aging increases prosocial motivation for effort. Psychol. Sci. 32 (5), 668–681.
MacPherson, S.E., Phillips, L.H., Sala, S.D., 2006. Age-related differences in the ability to perceive sad facial expressions. Aging Clin. Exp. Res. 18, 418–424.
Martin, A.K., Dzafic, I., Ramdave, S., Meinzer, M., 2017. Causal evidence for task-specific involvement of the dorsomedial prefrontal cortex in human social cognition. Soc. Cogn. Affect. Neurosci. 12 (8), 1209–1218.
Mather, M., 2012. The emotion paradox in the aging brain. Ann. N. Y. Acad. Sci. 1251 (1), 33–49.
Mather, M., 2016. The affective neuroscience of aging. Annu. Rev. Psychol. 67, 213–238.
Mathur, V.A., Harada, T., Lipke, T., Chiao, J.Y., 2010. Neural basis of extraordinary empathy and altruistic motivation. Neuroimage 51 (4), 1468–1475.
Mauchand, M., Zhang, S., 2023. Disentangling emotional signals in the brain: an ALE meta-analysis of vocal affect perception. Cogn. Affec. Behav. Neurosci. 23 (1), 17–29.
Meng, F., Meng, F., Cui, Y., Li, X., Huang, W., Xue, Q., Bai, Z., Wu, S., Xu, H., 2023. Neural mechanisms of social empathy in the anterior cingulate cortex. Adv. Neurol. 2 (1), 281.
Menon, V., Uddin, L.Q., 2010. Saliency, switching, attention and control: a network model of insula function. Brain Struc. Func. 214, 655–667.
Moore, R.C., Dev, S.I., Jeste, D.V., Dziobek, I., Eyler, L.T., 2015. Distinct neural correlates of emotional and cognitive empathy in older adults. Psych. Res.: Neuroimag. 232 (1), 42–50.
Namkung, H., Kim, S.-H., Sawa, A., 2017. The insula: an underestimated brain area in clinical neuroscience, psychiatry, and neurology. Trends Neurosci. 40 (4), 200–207.
Niu, L., Song, X., Li, Q., Peng, L., Dai, H., Zhang, J., Chen, K., Lee, T.M., Zhang, R., 2024. Age-related positive emotional reactivity decline associated with the anterior insula based resting-state functional connectivity. Hum. Brain Mapp. 45 (2), e26621.
Oosterhof, N.N., Connolly, A.C., Haxby, J.V., 2016. CoSMoMVPA: multi-modal multivariate pattern analysis of neuroimaging data in Matlab/GNU Octave. Front. Neuroinform. 10, 27.
Orlando, I., Filippini, N., 2024. Aging modulates frontal lobes involvement in emotion regulation processing. J. Neurosci. Res. 102 (1), e25282.
Pavuluri, M., May, A., 2015. I feel, therefore, I am: the insula and its role in human emotion, cognition and the sensory-motor system. AIMS Neurosci. 2 (1).
Piva, M., Velnoskey, K., Jia, R., Nair, A., Levy, I., Chang, S.W., 2019. The dorsomedial prefrontal cortex computes task-invariant relative subjective value for self and other. Elife 8, e44939.
Popal, H., Wang, Y., Olson, I.R., 2019. A guide to representational similarity analysis for social neuroscience. Soc. Cogn. Affect. Neurosci. 14 (11), 1243–1253.
Power, J.D., Mitra, A., Laumann, T.O., Snyder, A.Z., Schlaggar, B.L., Petersen, S.E., 2014. Methods to detect, characterize, and remove motion artifact in resting state fMRI. Neuroimage 84, 320–341.
Rogers-Carter, M.M., Christianson, J.P., 2019. An insular view of the social decision-making network. Neurosci. Biobehav. Rev. 103, 119–132.
Rosseel, Y., 2012. lavaan: an R package for structural equation modeling. J. Stat. Softw. 48, 1–36.
Ruffman, T., Henry, J.D., Livingstone, V., Phillips, L.H., 2008. A meta-analytic review of emotion recognition and aging: implications for neuropsychological models of aging. Neurosci. Biobehav. Rev. 32 (4), 863–881.
Schirmer, A., Adolphs, R., 2017. Emotion perception from face, voice, and touch: comparisons and convergence. Trends Cogn. Sci. (Regul. Ed.) 21 (3), 216–228.
Shamay-Tsoory, S.G., 2011. The neural bases for empathy. Neuroscientist 17 (1), 18–24.
Singer, T., Critchley, H.D., Preuschoff, K., 2009. A common role of insula in feelings, empathy and uncertainty. Trends Cogn. Sci. (Regul. Ed.) 13 (8), 334–340.
Small, D.A., Verrochi, N.M., 2009. The face of need: facial emotion expression on charity advertisements. J. Mark. Res. 46 (6), 777–787.
Song, X., Dong, M., Feng, K., Li, J., Hu, X., Liu, T., 2024. Influence of interpersonal distance on collaborative performance in the joint Simon task—An fNIRS-based hyperscanning study. Neuroimage 285, 120473.
Sun, F.W., Stepanovic, M.R., Andreano, J., Barrett, L.F., Touroutoglou, A., Dickerson, B. C., 2016. Youthful brains in older adults: preserved neuroanatomy in the default mode and salience networks contributes to youthful memory in superaging. J. Neurosci. 36 (37), 9659–9668.
Toga, A.W., 2015. Brain mapping: An encyclopedic Reference. Academic Press.
Tomova, L., Saxe, R., Klöbl, M., Lanzenberger, R., Lamm, C., 2020. Acute stress alters neural patterns of value representation for others. Neuroimage 209, 116497.
Treiber, J.M., White, N.S., Steed, T.C., Bartsch, H., Holland, D., Farid, N., McDonald, C. R., Carter, B.S., Dale, A.M., Chen, C.C., 2016. Characterization and correction of geometric distortions in 814 diffusion weighted images. PLoS ONE 11 (3), e0152472.
Tustison, N.J., Avants, B.B., Cook, P.A., Zheng, Y., Egan, A., Yushkevich, P.A., Gee, J.C., 2010. N4ITK: improved N3 bias correction. IEEE Trans. Med. Imaging 29 (6), 1310–1320.
Van Kleef, G.A., Lelieveld, G.-J., 2022. Moving the self and others to do good: the emotional underpinnings of prosocial behavior. Curr. Opin. Psychol. 44, 80–88.
Verstaen, A., Eckart, J.A., Muhtadie, L., Otero, M.C., Sturm, V.E., Haase, C.M., Miller, B. L., Levenson, R.W., 2016. Insular atrophy and diminished disgust reactivity. Emotion 16 (6), 903.
Vicario, C.M., Rafal, R.D., Martino, D., Avenanti, A., 2017. Core, social and moral disgust are bounded: a review on behavioral and neural bases of repugnance in clinical disorders. Neurosci. Biobehav. Rev. 80, 185–200.
Wagner, D.D., Kelley, W.M., Haxby, J.V., Heatherton, T.F., 2016. The dorsal medial prefrontal cortex responds preferentially to social interactions during natural viewing. J. Neurosci. 36 (26), 6917–6925.
Wang, S., Peterson, D.J., Gatenby, J.C., Li, W., Grabowski, T.J., Madhyastha, T.M., 2017. Evaluation of field map and nonlinear registration methods for correction of susceptibility artifacts in diffusion MRI. Front. Neuroinform. 11, 17.
Wever, M.C., van Houtum, L.A., Janssen, L.H., Will, G.-J., Tollenaar, M.S., Elzinga, B.M., 2021. Neural signatures of parental empathic responses to imagined suffering of their adolescent child. Neuroimage 232, 117886.
Wiepking, P., James, R.N., 2013. Why Are the Oldest Old Less generous? Explanations for the Unexpected Age-Related Drop in Charitable Giving, 33. Ageing & Society, pp. 486–510.
Xiao, W., Lin, X., Li, X., Xu, X., Guo, H., Sun, B., Jiang, H., 2021. The influence of emotion and empathy on decisions to help others. Sage Open 11 (2), 21582440211014513.
Xie, H., Karipidis, I.I., Howell, A., Schreier, M., Sheau, K.E., Manchanda, M.K., Ayub, R., Glover, G.H., Jung, M., Reiss, A.L., 2020. Finding the neural correlates of collaboration using a three-person fMRI hyperscanning paradigm. Proc. Natl. Acad. Sci. 117 (37), 23066–23072.
Zhang, F.-F., Dong, Y., Wang, K., 2010. Reliability and validity of the Chinese version of the interpersonal reactivity index-C. Chin. J. Clin. Psychol.
Zhang, Y., Brady, M., Smith, S., 2001. Segmentation of brain MR images through a hidden Markov random field model and the expectation-maximization algorithm. IEEE Trans. Med. Imaging 20 (1), 45–57.
Zhang, Y., Ye, W., Yin, J., Wu, Q., Huang, Y., Hao, N., Cui, L., Zhang, M., Cai, D., 2024. Exploring the role of mutual prediction in inter-brain synchronization during competitive interactions: an fNIRS hyperscanning investigation. Cereb. Cort. 34 (1), bhad483.
Zhang, Y., Zhou, W., Wang, S., Zhou, Q., Wang, H., Zhang, B., Huang, J., Hong, B., Wang, X., 2019. The roles of subdivisions of human insula in emotion perception and auditory processing. Cereb. Cort. 29 (2), 517–528.
Zhao, Q., Zhao, W., Lu, C., Du, H., Chi, P., 2024. Interpersonal neural synchronization during social interactions in close relationships: a systematic review and meta-analysis of fNIRS hyperscanning studies. Neurosci. Biobehav. Rev., 105565
Ziaei, M., Oestreich, L., Reutens, D.C., Ebner, N.C., 2021. Age-related differences in negative cognitive empathy but similarities in positive affective empathy. Brain Struc. Func. 226, 1823–1840.